19th International Conference
ENGINEERING MECHANICS 2013
Svratka, Czech Republic, May 13 – 16, 2013

DAMPING OF BEAM TRANSVERSAL VIBRATIONS BY A PERMANENT MAGNET WITH COIL

G. J. Stein*, R. Chmúrny*

Abstract: *In the paper the use of permanent magnet with coil, augmented by an external resistance, for transversal vibration control of a flexible slender beam is analysed. The magnetic circuit properties are varied due to external harmonic excitation by a rotating machine. The so induced alternating voltage drives alternating current through closed electric circuit, which is dissipated in external resistor. The induced current driven through the coil generates magnetic force, which damps the excitation force and changes the damped natural frequency of the oscillatory system. The internal losses in the coil influence the overall system's performance. A lumped parameter model of the combined system is derived in a simplified, linearised form for a particular machine frame, using measured system parameters. The extent of system natural frequency shift is assessed.*

Keywords: ***Vibration control assessment, Electromagnetic actuator, Harmonic excitation, Numerical simulation.***

1. Introduction

Many of the vibration control problems of rotating machinery are associated with various resonance phenomena in the machine frame. To avoid interaction of the rotating machine dominant rotating frequencies and their harmonics with eigenfrequencies of the supporting structure following methods are in general used:

- detuning of the frame eigenfrequencies from the range of machine operational frequencies;
- introduction of additional damping to the (usually low) structural damping of the frame.

Recently, some active and semi-active methods of vibration control were explored. Electro-dynamic and electro-magnetic actuators were used for such a control strategy as presented in (Bishop, 2002; Giurgiutiu & Lyshewski, 2009; Preumont, 2011). Some applications of vibration control of cantilever beams using electromagnetic and electrodynamic vibration controllers were published by Gospodarič et al. (2007); Cheng & Oh (2009); Niu, Xie & Wang (2009); Brezina et al. (2011) and Belhaq et al. (2011). Especially Xu and Zhu (2010) used an electro-magnetic actuator for driver's seat vibration control.

This contribution, based on first author's previous works (Stein et al., 2011; Stein et al., 2012), analyses the use of a permanent magnet with a coil for similar purpose. It has been shown therein that the controller of interest is capable to introduce damping, as well as alter damped natural frequency of the oscillatory system. In order to model more realistic system, particular parameters of a dummy system are used in here. The system mocks-up a real rotating machine, situated on the frame (chassis).

2. Description of the analysed system

The contribution describes the use of an industrial pot type magnet with a ferromagnetic yoke fixed in the middle of a diamagnetic slender beam of length l, mass m, ideally clamped at the ends. The beam represents the machine frame. A static magnetic field is generated by the permanent magnet (PM), located in the centre of a coil. As the yoke vibrates due to the influence of the harmonic force $F_E(t)$, the air gap width $d(t)$ varies with time. The variation of $d(t)$ is responsible for time variation of the air

* Ing. George Juraj Stein, PhD. and Ing. Rudolf Chmúrny, PhD.: Institute of Materials and Machine Mechanics, Slovak Academy of Sciences, Račianska 75, SK-831 02, Bratislava; Slovakia, e-mail: stein@savba.sk and ummschmu@savba.sk

gap reluctance and consequently for the primary magnetic flux time variations. According to Faraday's law, magnetic flux time variation induces alternating voltage $u(t)$ in the coil. The induced voltage forces a current $i(t)$ flowing in the closed electrical circuit. The direction of $i(t)$ is such that so generated secondary magnetic field opposes the primary field of the PM (Lenz's law). The alternating magnetic force, due to the induced current, acts both as a damping and a spring force. The current $i(t)$ is dissipated in the shunt resistance R_T, which includes also all the electrical losses in the coil. The combination of the static magnetic force F_{M0} of the PM and the dynamic one $F_M(t)$ influences the structure stiffness and thus the natural frequency. Moreover, the induced current $i(t)$ intensity influences the extent of damping.

3. Simplified derivation of the magnetic field influence

As assumed, a periodic force $F_E(t)$ is exciting the clamped-clamped, slender beam at its midpoint. Due to force $F_E(t)$ the air gap width $d(t)$ between the yoke and the core is periodically varying, thus generating an alternating magnetic induction $B(t)$ in the air gap. According to Faraday's law of induction, in the coil of cross-section S_W and number of turns N, alternating voltage $u_i(t)$ is generated:

$$u_i(t) = -\frac{d\Phi}{dt} = -NS_W\frac{dB(t)}{dt} = i(t)\cdot R_T, \tag{1}$$

where: - $\Phi = N\,S_W\,B(t)$ is the total magnetic flux in the opened magnetic circuit,
- $i(t)$ is the alternating induced current flowing through the closed electrical circuit,
- R_T is the total electric resistance of the closed circuit (including coil losses).

The magnetic circuit consists, according to Hopkinson's law, of series connection of the reluctances of the air gap (twice), the pot core, the yoke and of the PM itself. Assuming constant core cross-section S_C and neglecting fringing effects and core/yoke material magnetic non-linearity, it can be derived (Giurgiutiu & Lyshewski, 2009; Meyer & Ulrych, 2009):

$$\Phi(t) = \frac{F_\Phi(t)}{\sum R_M(t)} = \frac{F_\Phi(t)}{\frac{1}{S_C\mu_0}\left[l_g(t) + \frac{l_C}{\mu_{rFe}} + \frac{l_{PM}}{\mu_{rPM}}\right]} = \frac{F_\Phi(t)}{l_{\Phi r}}, \tag{2}$$

where l_C, l_g, and l_{PM} are in turn the length of the flux line in the core/armature of relative permeability μ_{rFe}, of the air gap and of the PM, with material relative permeability μ_{rPM}, respectively. $F_\Phi(t)$ is the magnetomotive force in the said magnetic circuit, which has a steady state component, due to the PM, and a time varying component, due to the alternating current $i(t)$, as it follows from the Ampere's circuital law (Meyer & Ulrych, 2009):

$$F_\Phi = \oint_C \vec{H}\cdot d\vec{L} = M_m + Ni(t), \tag{3}$$

where the contour integral over the closed curve C follows the middle magnetic flux line of length in air $l_{\Phi r}$, depicted dashed in Fig. 1, and M_m is the PM magnetisation.

Introducing the scaled dimensions $d_C = l_C/(2\mu_{rC})$, $d_{PM} = l_{PM}/(2\mu_{rPM})$, $2(d(t) - d_0) = l_g$ and the non-dimensional parameter $\delta = (d_C + d_{PM})/d_0$, then, according Stein et al. (2011), it follows:

$$B(t) = \frac{\mu_0}{2d_0}\frac{\left[M_m + Ni(t)\right]}{\left[(1+\delta) + \varepsilon(t)\right]}, \tag{4}$$

where:
- d_0 is the equilibrium distance between yoke and the PM,
- $w(t)$ is the dynamic displacement of the yoke from the equilibrium position d_0: $w(t) = d(t) - d_0$ in the positive (upwards) direction,
- $\varepsilon(t)$ is the relative dynamic displacement: $\varepsilon(t) = w(t)/d_0$, positive in the upward direction, further referred to as the relative air gap width (a non-dimensional quantity).

It will be further assumed that $|w(t)| << d_0$, i.e. $|\varepsilon(t)| << 1$.

Eq. (4) represents the general form of magnetic induction in the air gap in the time domain. If the electrical circuit is not closed, no current is flowing and the last term in numerator is zero. There is no oscillating magnetic field and just the static magnetic field in the air gap, B_0 is present, due to PM magnetisation M_m:

$$B_0 = \frac{\mu_0}{2d_0}\frac{M_m}{(1+\delta)} = \text{const}(d_0)\,. \tag{5}$$

Substituting from Eq. (1) into Eq. (3) for the induced current $i(t)$, it follows:

$$F_\Phi(t) = M_m + Ni(t) = M_m - \frac{N^2 S_W}{R_T}\frac{dB(t)}{dt}\,, \tag{6}$$

and:

$$B(t) = \frac{\mu_0}{2d_0}\frac{\left[M_m - \frac{N^2 S_W}{R_T}\frac{dB(t)}{dt}\right]}{\left[(1+\delta)+\varepsilon(t)\right]}\,. \tag{7}$$

Now, when all the characteristics of the electro-magnetic circuit have been derived the magnitude of the magnetic force F_M acting onto the yoke downwards can be expressed. Hence, in this particular case (Meyer & Ulrych, 2009):

$$F_M(t) = 2\times\frac{1}{2\mu_0}B(t)^2 S_C\,, \tag{8}$$

because the Maxwell's magnetic pulling force is acting both at the inner core and at outside annulus, both having the same cross-section S_C. After substitution from Eqs. (7) and (5):

$$F_M(t) = \frac{1}{\mu_0}B(t)^2 S_C = \frac{\mu_0 S_C}{4d_0^2}\frac{\left[M_m + i(t)N\right]^2}{\left[(1+\delta)+\varepsilon(t)\right]^2} = \frac{\mu_0 S_C}{4d_0^2}\frac{F_\Phi(t)^2}{\left[(1+\delta)+\varepsilon(t)\right]^2}\,. \tag{9}$$

Note, that the magnetic force $F_M(t)$ due to squared magnetic induction has a non-linear form and hence is difficult to calculate. Some simplifications have to be made. Moreover, the time variation of the magnetic induction $B(t)$ in the air gap has to be evaluated, too.

Let us first consider $|\varepsilon| << 1$. Then the acting magnetic force F_{MO} can be approximated by linearization in respect to variable ε, i.e. taking the first two term of a MacLaurin expansion:

$$F_{MO}(\varepsilon) \cong \frac{\mu_0 S_C}{4d_0^{\,2}}\frac{F_\Phi^{\,2}}{(1+\delta)^2} - \frac{\mu_0 S_C}{2d_0^{\,2}}\frac{F_\Phi^{\,2}}{(1+\delta)^3}\varepsilon(t)\,. \tag{10}$$

As derived in (Stein et al., 2011) the total differential of magnetic induction $B(t)$ can be calculated from Eq. (4) as:

$$\frac{dB(t)}{dt} = \frac{\partial B}{\partial \varepsilon}\frac{d\varepsilon}{dt} + \frac{\partial B}{\partial i}\frac{di}{dt} = \frac{\partial B}{\partial \varepsilon}\dot{\varepsilon} - \frac{\mu_0 N^2 S_W}{2d_0(1+\delta)R_T}\frac{d^2 B(t)}{dt^2}\,. \tag{11}$$

By further algebraic manipulations it results, that the time dependence of the variable magnetic induction is described by a first order differential equation in dB/dt in respect to $\dot{\varepsilon}$:

$$\frac{d^2B(t)}{dt^2}\left[\frac{\mu_0 N^2 S_W}{2d_0(1+\delta)}\right]\frac{1}{R_T}+\frac{dB(t)}{dt}=-\frac{B_0}{(1+\delta)}\dot{\varepsilon}\,. \tag{12}$$

The term in the square bracket is the self inductance L_0 of the coil at air gap d_0 and B_0 is the static magnetic induction in the air gap width d_0, as introduced above by Eq. (5).

Note, there is a difference in the areas S_W (cross-section of the coil) and S_C (cross-section of the core). However, because the magnetic flux is flowing mainly through the ferromagnetic core with relative permeability $\mu_{rC} >> 1$, it can be assumed that $S_W \approx S_C$.

The total resistance R_T in the electric circuit consists of the series combination of the external shunt resistance R_S, internal resistance of the coil R_C and the resistor R_L, which is used to model the frequency dependent losses in the magnetic material. The series equivalent circuit of a technical coil is used, so the resistances R_C and R_L are connected in series with the coil inductance L_0:

$$R_T(\omega)=R_S+R_C+R_L(\omega)\,. \tag{13}$$

No eddy currents are acting in this specific configuration, because the beam velocity vector $\vec{v}$ has the same direction as the vector of the magnetic induction $\vec{B}$ giving a zero vector product $\vec{v}\times\vec{B}$, entering the expression for the Lorenz force, which describes the eddy currents in conductors subjected to magnetic field.

4. Simplified derivation of the magnetic force influence

The influence of the magnetic force in the air gap plays a decisive role in the analysed system description. Let us start with analysis of the mechanical part of the system.

4.1. Static analysis

Firstly, let us analyse the static deflection of a slender beam of length *l*, mass *m* rigidly fixed on both ends, loaded at beam midpoint by the mass of the yoke and a the supposed machine, jointly of mass *M*, without the presence of the PM. Let us assume, that the machine can be represented by a concentrated mass *M* at the beam midpoint. Using the standard expression of equivalent (lumped) stiffness for the clamped-clamped beam, the small deflection, h_S at the beam midpoint from a straight line due to mass *M* is (Bishop, 2002; Stein et al., 2011 and 2012):

$$h_S=(Mg_N)\cdot\left(\frac{1}{192}\frac{l^3}{E_Y I_b}\right), \tag{14}$$

where E_Y is the modulus of elasticity (Young's module) of the beam material and I_b is the second moment of inertia of the beam cross-section. The weight, given by the first coefficient, bends the beam from an ideal straight form a little. The second coefficient is the inverse of the equivalent bending stiffness of the beam, k_S at beam midpoint.

Let us now locate the PM below the bent beam midpoint. Same formula holds for the static deflection by the magnetic force F_M; however, the first term in Eq. (14) is substituted by the static magnetic force F_{M0} (Stein et al., 2012):

$$F_{M0}=\frac{\mu_0 S_C}{4d_0^2}\frac{M_m^2}{(1+\delta)^2}\,, \tag{15}$$

where d_0 is the static distance between the yoke and upper plane of the core.

As seen from Fig. 1, the magnetic force F_{M0} is counteracted by the static elastic spring force F_S. If F_{M0} were to overwhelm F_S, the yoke would be permanently attracted to the PM and any oscillatory motion would cease. This situation has to be avoided. Let us define a fictitious distance *h* between the yoke of the statically bent beam and the upper plane of the PM core in the virtual absence of the magnetic field. If now the magnetic field of the PM is accounted for, the spring would elongate and the yoke would reach an equilibrium position at a distance $d_0 < h$. When the distance *h* is slowly

reduced, at a certain distance h_L the magnetic force would overwhelm the elastic force and permanent attraction would occur, i.e. d_0 would become zero. Let us describe the specific d_{0L} just before this instant in respect to h_L as $d_{0L} = h_L(1 - \varepsilon_s)$, where ε_s is a downward relative static displacement from h_L ($0 < \varepsilon_s < 1$). The static equilibrium is then expressed using equation (15) (Stein et al., 2012):

$$\frac{\mu_0 S_C}{4h_L^2}\frac{M_m^2}{\left[(1+\delta)-\varepsilon_s\right]^2} = k_S(h_L - d_{0L}) = k_S h_L \varepsilon_s . \tag{16}$$

Equation (16) leads to a cubic equation in ε_s:

$$\varepsilon_s^3 - 2\varepsilon_s^2(1+\delta) + \varepsilon_s(1+\delta)^2 - \left(\frac{\mu_0 S_C}{4h_L^3}\frac{M_m^2}{k_S}\right) = 0 . \tag{17}$$

Equation (17) has three real roots, if its discriminator $D_3 \geq 0$ (Frank et al., 1973). From the solution of the equation (17) follows, that this condition is fulfilled if:

$$\frac{1}{h_L^3(1+\delta)^3}\frac{\mu_0 S_C M_m^2}{k_S} \leq \frac{16}{27} . \tag{18}$$

The equality case corresponds to the sought limiting case. The three real roots for $D_3 = 0$ are: $\varepsilon_{s1} = \varepsilon_{s2} = (1+\delta)/3 < 1$ and $\varepsilon_{s3} = 4/3(1+\delta) > 1$. This result can be physically interpreted that either the system is just at equilibrium at a particular distance or it should be within the magnetic circuit core, which is physically impossible. Hence, this is the limiting case of the 'jump' from the stable oscillatory mode to the fully attracted mode, albeit neglecting any system dynamics and/or mechanical transitions. The total magnetic flux line length in air $l_{\Phi r}$ for this case should follow the inequality:

$$\left(\frac{l_{\Phi r}}{2}\right)^3 = h_L^3(1+\delta)^3 = (h_L + d_C + d_{PM})^3 \geq \frac{27}{16}\frac{\mu_0 S_C M_m^2}{k_S} . \tag{19}$$

For a particular PM, magnetic circuit parameters and spring stiffness k_S, the limiting value h_S can be assessed for the equality in Eq. (19). However, the yoke will be positioned at the distance $d_{0L} = h_L(1 - \varepsilon_{S1})$ from the original beam position without the influence of the magnetic field. The measurable distance between the yoke and the upper plane of the core, d_{0L}, is for the limiting case:

$$d_{0L} = \frac{h_L}{3}(1+\delta) = \frac{1}{2}\sqrt[3]{\frac{\mu_0 S_C M_m^2}{2k_S}} . \tag{20}$$

In practice, any air gap width $d_0 \geq d_{0L}$ can be used without jeopardising the vibration control.

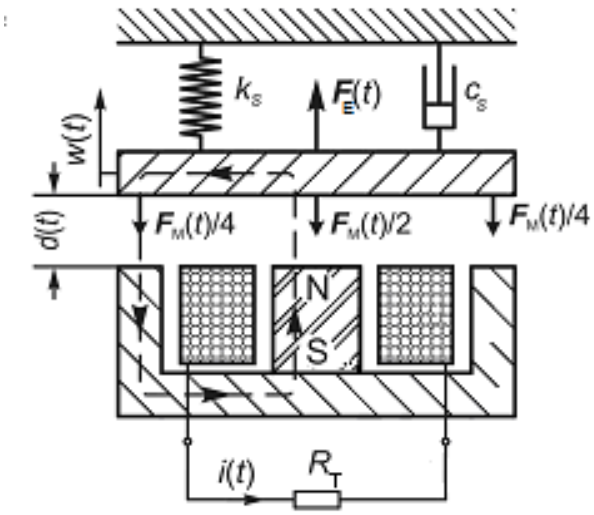

Fig. 1: Equivalent SDOF oscillatory system.

4.2. Description of the system dynamics

For sake of simplicity, the beam is modelled as a single degree-of-freedom (SDOF) oscillatory system subjected to a harmonic excitation force $F_E(t)$. As described above, additional magnetic force $F_M(d_0,i(t))$ is generated. The governing equation is hence:

$$M\ddot{w} + c_S\dot{w} + k_S w = F_E(t) - F_M(d_0, i(t)), \tag{21}$$

where:

- M is the mass of the yoke and mass of the machine,
- c_S is the viscous damping coefficient, modelling the internal damping of the beam,
- k_S is the equivalent beam stiffness at its midpoint,
- w is is the midpoint displacement in the upward direction and its time derivatives.

Introducing the relative air gap width $\varepsilon(t)$ and the natural frequency of the equivalent oscillatory system ω_0, ($\omega_0^2 = k_S/M$); being approximately beam first eigenfrequency (Harris & Creede, 1961):

$$\ddot{\varepsilon} + \left(\frac{c_S}{M}\right)\dot{\varepsilon} + \omega_0^2\varepsilon = \frac{F_E(t)}{Md_0} - \frac{F_M(t)}{Md_0}. \tag{22}$$

The response of the system is analyzed under steady state condition, while the exciting harmonic force is $F_E(t) = F_0\sin(\omega t)$ of angular frequency ω, expressed, using the complex notation, as $F_E(t) = F_0\mathrm{Re}\{\exp(\mathrm{j}\omega t)\}$. It is assumed, that all transient phenomena (electric and mechanic) are extinct. Assuming, that the response will be harmonic too, the complex relative air gap width $\tilde{E}$ will be expressed as $\tilde{E}e^{\mathrm{j}\omega t} = \varepsilon_0 e^{\mathrm{j}\varphi_\varepsilon}e^{\mathrm{j}\omega t}$. Then:

$$\left[1 - \Omega^2 + 2\mathrm{j}\xi_S\Omega\right]\tilde{E}e^{\mathrm{j}\omega t} = \frac{\tilde{F}_0 e^{\mathrm{j}\omega t}}{k_S d_0} - \frac{\tilde{F}_{MO}}{k_S d_0}, \tag{23}$$

where:

- $\Omega = \omega/\omega_0$ is the non-dimensional frequency ratio,
- $\xi_S = c_S/c_C$ is the damping ratio with $c_C = 2\sqrt{k_S M}$ being the critical damping coefficient.

The term in the square brackets on the left hand side is a linear second order operator, describing the behaviour of the SDOF oscillatory system without the influence of the PM magnetic field. The normalized displacement response of the uncontrolled mechanical SDOF oscillatory system $\tilde{E}_0$ can be evaluated for any external harmonic excitation force F_E by setting $\tilde{F}_{MO} = 0$.

The magnetic force, is in linearised, approximate form given by Eq. (10). It can be expressed in the frequency domain as:

$$\tilde{F}_{MO} = \sum_{n=0}^{Q}\tilde{F}_{Mn}e^{\mathrm{j}n\omega t} = \frac{\mu_0 S_C}{4d_0^2}\frac{\tilde{F}_\Phi^{\,2}}{(1+\delta)^2} - \frac{\mu_0 S_C}{2d_0^2}\frac{\tilde{F}_\Phi^{\,2}\cdot\tilde{E}e^{\mathrm{j}\omega t}}{(1+\delta)^3}. \tag{24}$$

Due to the square of the magnetomotive force phasor, $\tilde{F}_\Phi$, the magnetic force acts at Q multiple harmonics of the excitation frequency ω. From Eq. (6):

$$\left(\tilde{F}_\Phi\right)^2 = M_m^2 - \mathrm{j}\frac{2M_m\omega N^2 S_C}{R_T}\tilde{B} - \frac{\omega^2 N^4 S_C^2}{R_T^2}\left(\tilde{B}\right)^2, \tag{25}$$

where, the time derivation of magnetic induction phasor, $\tilde{B}$, was performed in the frequency domain.

The magnetic induction phasor $\tilde{B}$ is evaluated from Eq. (12) by applying the Fourier transform. After some algebraic manipulation it follows:

$$\tilde{B} = -\frac{B_0 R_T}{(1+\delta)(R_T + \mathrm{j}\omega L_0)}\tilde{E}. \tag{26}$$

Further inserting B_0 from Eq. (5) and noting the definition of inductance L_0 from Eq. (12), the magnetomotive force F_Φ of Eq. (25) is expressed as:

$$\left(\tilde{F}_\Phi\right)^2 = M_{\mathrm{m}}^2 + \mathrm{j}\frac{2\,\omega L_0 M_{\mathrm{m}}^2}{(1+\delta)(R_{\mathrm{T}} + \mathrm{j}\omega L_0)}\tilde{E} - \left(\frac{\omega L_0 M_{\mathrm{m}}^2}{(1+\delta)(R_{\mathrm{T}} + \mathrm{j}\omega L_0)}\right)^2 \tilde{E}^2 . \quad (27)$$

Looking at Eqs. (24) and (27) it can be qualitatively stated that after performing the multiplications and some algebraic re-arrangement following magnetic force components emerge Stein et al. (2012):

- *a static component for* $n = 0$, affecting the equilibrium position at d_0 and so the static magnetic induction B_0 (see Eq. (15)):

$$F_{\mathrm{M0}} = \frac{\mu_0 S_{\mathrm{C}} M_{\mathrm{m}}^2}{4 d_0^2 (1+\delta)^2} = \left(\frac{\mu_0 S_{\mathrm{C}} M_{\mathrm{m}}^2}{2 d_0^3 (1+\delta)^3}\right)\cdot\frac{d_0(1+\delta)}{2} . \quad (28)$$

  As derived above, the static magnetic force F_{M0} must be smaller than F_{S}, else the beam clams to the PM and any oscillatory movement ceases. There is limit on the distance d_0, as explained.

- *a component at the angular frequency* ω *(n = 1)*, contributing to the equation of motion

$$\tilde{F}_{\mathrm{M1}} = \left(\frac{\mu_0 S_{\mathrm{C}} M_{\mathrm{m}}^2}{2 d_0^3 (1+\delta)^3}\right)\cdot\frac{\mathrm{j}\omega L_0}{(R + \mathrm{j}\omega L_0)}\cdot d_0\tilde{E} - \left(\frac{\mu_0 S_{\mathrm{C}} M_{\mathrm{m}}^2}{2 d_0^3 (1+\delta)^3}\right)\cdot d_0\tilde{E} . \quad (29)$$

  Both terms give relation between the relative air gap phasor $\tilde{E}$ and the magnetic force component phasor $\tilde{F}_{M1}$.

- *a second harmonic component* at the angular frequency $2\times\omega$ ($n = 2$), which is well known to be associated with magnetic circuits (Bishop, 2002; Giurgiutiu & Lyshewski, 2009). However, in the case of clamped-clamped beam excited at the midpoint, i.e. in the antinode, no mechanical effect could result.

- *a third harmonic component* at the angular frequency $3\times\omega$ ($n = 3$). However, being of the order of $|\varepsilon|^3$ it can be assumed that it does not markedly influence the system behaviour.

Note, that in Eq. (28) and (29) the same factor (highlighted in the brackets), related to the magnetic circuit properties, occurs. The factor in the brackets can be termed the equivalent, linearised magnetic field stiffness at air gap width d_0, k_{M}. Then the Eq. (29) can be modified and introduced into Eq. (23), to arrive at the system behaviour at excitation frequency ω.

$$\left[1 - \Omega^2 + 2\mathrm{j}\zeta_{\mathrm{S}}\Omega\right]\cdot\tilde{E} = \frac{\tilde{F}_{\mathrm{E}}}{k_{\mathrm{S}} d_0} + \frac{k_{\mathrm{M}}}{k_{\mathrm{S}}}\frac{(R_{\mathrm{T}}^2 - \mathrm{j}\omega L_0 R_{\mathrm{T}})}{R_{\mathrm{T}}^2 + \omega^2 L_0^2}\cdot\tilde{E} . \quad (30)$$

Introducing the stiffness ratio κ ($\kappa = k_{\mathrm{M}}/k_{\mathrm{S}}$) and the coil reactance X_0 at the mechanical system natural frequency ω_0: $X_0 = \omega_0 L_0$, Eq. (30) can be further modified to become:

$$\left\{\left[1 - \kappa\frac{R_{\mathrm{T}}^2}{\left(R_{\mathrm{T}}^2 + \Omega^2 X_0^2\right)}\right] - \Omega^2 + 2\mathrm{j}\Omega\left[\zeta_{\mathrm{S}} + \frac{\kappa}{2}\frac{X_0 R_{\mathrm{T}}}{\left(R_{\mathrm{T}}^2 + \Omega^2 X_0^2\right)}\right]\right\}\tilde{E} = \frac{\tilde{F}_{\mathrm{E}}}{d_0 k_{\mathrm{S}}} . \quad (31)$$

The displacement response of the oscillatory system, $\tilde{E}$, can be now evaluated from Eq. (31) and compared to the response of the uncontrolled mechanical system $\tilde{E}_0$. In particular (Stein et al., 2011):

- There is a change (decrease) of the angular frequency ω_{C}, describing the natural frequency of the system with the PM, in respect to the natural frequency ω_0 of the uncontrolled SDOF mechanical system:

$$\omega_{\mathrm{C}} = \omega_0\sqrt{1 - \kappa\frac{R_{\mathrm{T}}^2}{(R_{\mathrm{T}}^2 + \Omega^2 X_0^2)}} , \quad (32)$$

  which, for the given air gap width d_0, depends on the properties of electrical circuit (total circuit resistance R_{T} and coil self inductance L_0).

- Additional electro-magnetic damping is introduced, which can be described by electro-magnetic damping ratio ζ_E:

$$\zeta_E = \frac{\kappa}{2} \cdot \frac{X_0 R_T}{(R_T^2 + \Omega^2 X_0^2)}, \tag{33}$$

again depending for the air gap width d_0 on the electrical circuit properties. As discussed in more detail in (Stein et al., 2011), there is an optimal value of the total resistance R_T, equal to X_0, when the maximum of electromagnetic damping is attained.

The dimension-less factor κ, describing the magnetic circuit properties, is:

$$\kappa = \frac{\mu_0 S_C M_m^2}{2k_S (d_0 + d_C + d_{PM})^3} = \frac{4\mu_0 S_C M_m^2}{k_S l_{\Phi r}^3}. \tag{34}$$

Note, that from the inequality (19) follows, that at most $\kappa = k_M/k_S = 16/27 \approx 0.59$, to facilitate proper functioning of the vibration control system.

To conclude, the introduction of a PM with coil and external resistance, located at midpoint of the clamped-clamped beam at a distance d_0 below introduces additional (electro-dynamic) damping into the oscillatory system and decreases the natural frequency of the combined system. Both effects depend on the magnetic and electric properties of the device. Moreover, the static equilibrium position of the beam is modified, too.

5. Preliminary experimental determination of the system parameters

The electro-magnetic properties of the particular PM with coil, type GMPX 050 of the Magnet Schulz Company, Memmingen, Germany were measured for various air gap widths: 0.22 mm, 0.45 mm, 0.90 mm and 1.35 mm, using the automatic RLC meter of type Hioki IM 3570. For all air gap widths the DC coil resistance was $R_C = 17.0\ \Omega$. The core cross-section is, according to manufacturer's drawing, $S_c = 4.41\times10^{-4}$ m^2.

It was observed, that the coil resistance, R_L, as well as coil reactance X_0 are frequency and air gap dependent (Fig. 2).

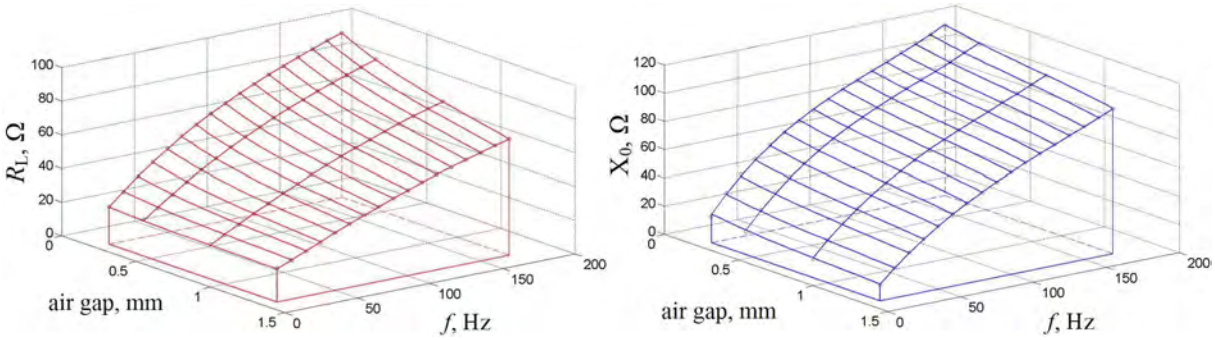

(a) (b)

Fig. 2: Frequency and gap width dependence of: (a) coil resistance $R_L(\omega)$, (b) coil reactance $X_0(\omega)$.

Another issue is the behaviour of the magnetic circuit, best expressed as the static force F_{M0} dependence on air gap width d_0 (Eq. (15) or (28)). However, some variables are not readily available, nor given in the manufacturer's data. Hence, the dependence had to be established experimentally. For this purpose a test stand was manufactured, enabling to move the PM in the vertical direction. The combination of the yoke weight and the magnetic force was measured by a force transducer, type LCM101, manufactured by Omega Engineering, Stamford, Con., USA; while the distance d_0 was determined by a set of plastic foils of thickness 0.22 mm. Because the force transducer was sensitive both to pull and to compression a somehow tricky adjustment was necessary to arrive at the exerted force. Given the circumstance, the relation between F_{M0} and d_0 was measured with low accuracy, assessed at some 5 % of the measured value. From Eq. (28) follows, after algebraic manipulation:

$$\sqrt{\frac{\mu_0 S_C}{4F_{M0}}} = \frac{l_{\Phi r}}{2M_m} = \frac{(d_C + d_{PM})}{M_m} + \frac{d_0}{M_m} = \alpha + \beta d_0, \tag{35}$$

wherefrom the unknown parameters ($d_C + d_{PM}$) and magnetisation M_m can be identified by the least squares method. The course of preliminary measurements of the static magnetic force F_{M0} in respect to air gap width d_0 is depicted in Fig. 3. Notice, that despite of linearity of formula (35) the measured points are not situated on straight line. This deviation is due to measurement uncertainty and due to magnetic field deviations from linearity, stipulated by the Hopkinson's law (Eq. (2)). Hence, just some air gap widths will be considered, approximated in Fig. 3 by the red line. From formula (35) it follows that ($d_C + d_{PM}$) = 0.165 mm and M_m = 120 A.

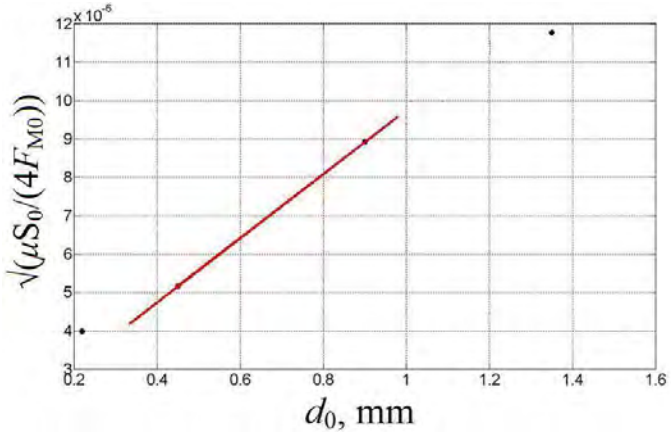

Fig. 3: Graphical presentation of formula (35).

Further issue is the equivalent beam stiffness for midpoint deflection k_S. According to Eq. (14) k_S can be evaluated by calculation from chassis geometry and material properties or by measurement of chassis deflection under stipulated load. Because the chassis has a rather complicated cross section profile, made of pressed steel sheet of thickness 0.3 mm and width 100 mm of length l = 554 mm between the fixtures and mass m = 474 g, the second moment of inertia of the beam cross-section calculation was deemed as imprecise. Hence, the midpoint deflection under a rigid load was measured by a dial indicator. The measured deflection due to rigid load of 6.925 kg was 0.96 mm leading to beam static stiffness of $k_S = 7.08 \times 10^4$ N/m.

6. Simulation results for the analysed case

Eq. (31) was programmed in Matlab®, loaded by stipulated machine mass M = 7 kg at chassis midpoint. For the evaluated beam equivalent stiffness $k_S = 7.08 \times 10^4$ N/m the undamped natural frequency of the equivalent SDOF oscillatory system is some $\omega_0 \approx 100$ rad/s, i.e. 16 Hz. Let us assume mechanical damping ratio ξ_S = 0.03, excitation force F_0 = 20 N. From Fig. 3 the parameters of the PM coil can be assessed for various air gap widths. The data extracted from measurements for frequency f_0 = 16 Hz and used in the following simulation are condensed in the Tab. 1.

Tab. 1: Numerical values entering the simulation and R_S optimization.

d_0 [mm]	R_L [Ω]	X_0 [Ω]	$\|Z_T\|$ [Ω]	$\|Z_T^*\|$ [Ω]
0.45	7.8	24.2	34.7	34.1
0.70*	6.9	22.0	32.4	31.0
0.90	6.2	20.3	30.9	28.6

* assessed by linear interpolation from measured data

The last two columns indicate the calculated modulus of the coil impedance at frequency 16 Hz: $|Z_T| = \sqrt{(R_L + R_C)^2 + X_0^2}$ and the measured impedance $|Z_T^*|$, interpolated from tabulated data. Note a good agreement of both values.

For illustration the projection of the course of the FRF response modulus $|\tilde{E}|$, according to Eq. (31), for the air gap width d_0 = 0.70 mm in respect to the circuit resistance for the idealised case of loss-less inductance is presented in Fig. 4. The same projection; however accounting for the measured coil losses is presented in Fig. 5. In Fig. 4 the blue curve depicts the course of the FRF modulus maximum, while the green course depicts the FRF for the optimum R_S, when the electro-dynamic damping is maximal. For the particular device this occurs in ideal case for $R_s = X_0$ = 22 Ω, as follows from Stein et al. (2011). In Fig. 5 the course of FRF modulus maximum for the real device is depicted in red; however, starting at R_S = 0, i.e. for R_T = 22.9 Ω. From comparison of these two figures the difference between the ideal, loss-less coil and real coil is visible. It follows, that optimal damping can be obtained if $|Z_T| = \sqrt{2}\cdot X_0$ (Stein et al., 2011). For the particular PM with coil the difference between the optimal electric circuit impedance $\sqrt{2}\cdot X_0 \approx 31.1$ Ω and the measured impedance $|Z_T^*| \approx 31.0$ Ω is diminutive. The same holds for the other two air gap widths. Hence, to obtain the most electro-dynamic damping out of the actuator the coil has to be short-circuited.

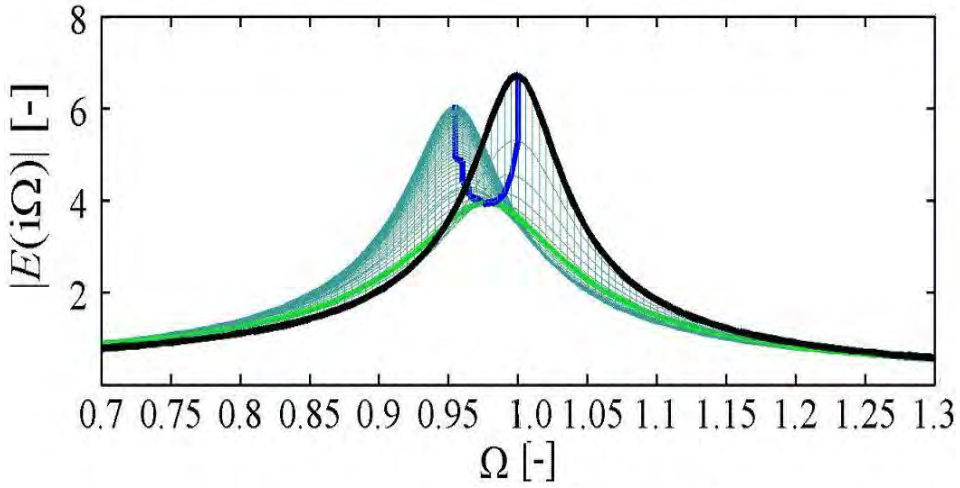

Fig. 4: Projection of the FRF modulus of ideal, loss-less coil in respect to shunt resistance R_S ($R_S \in (0, 200\ \Omega)$).

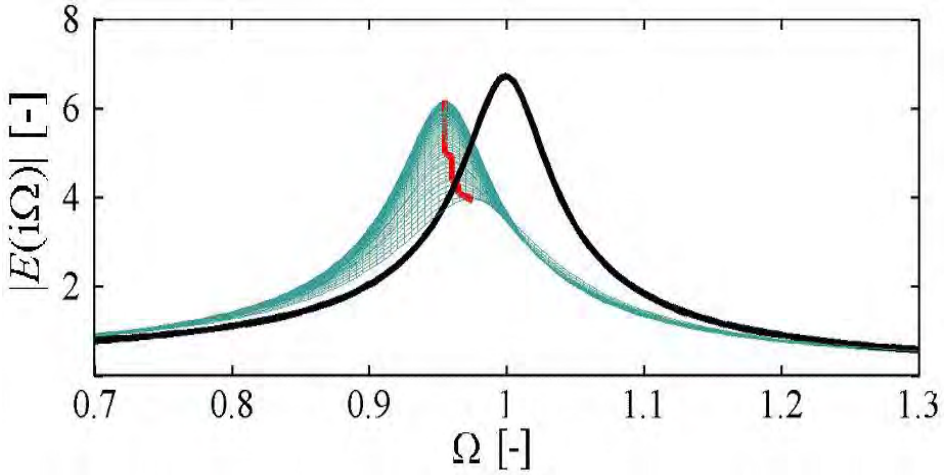

Fig. 5: Projection of the FRF modulus of the real coil in respect to shunt resistance R_S ($R_S \in (0, 200\ \Omega)$).

Next the extent of de-tuning in respect to variation in the air gap width d_0 is illustrated in Fig. 6 for the real coil and stipulated external resistance R_s = 500 Ω. Because on the right hand-side of Eq. (31) the air gap width d_0 is in denominator it is necessary to normalise the response modulus $|\tilde{E}|$ in respect to same air gap width; specifically in this case to d_0 = 0.70 mm. The attained frequency shift of the FRF maximum in respect to the uncontrolled system is by some 13 %, i.e. to Ω = 0.87.

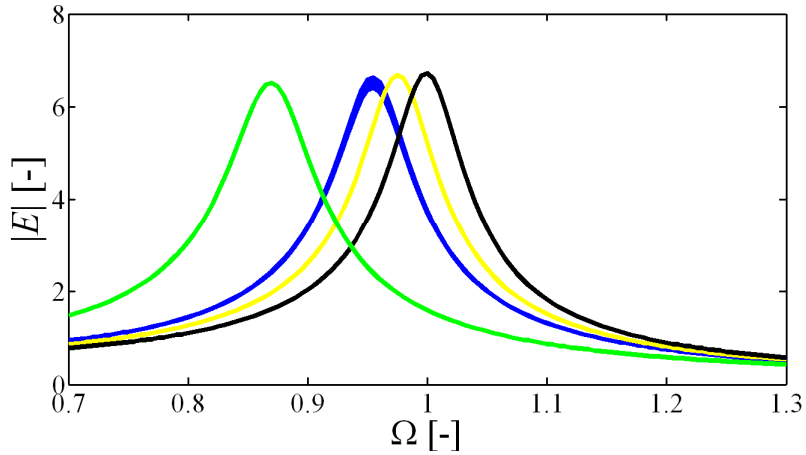

Fig. 6: The FRF modulus of real coil for R_S = 500 Ω in dependence on the air gap width d_0, normalized to d_0 = 70 mm (d_0 = 0.45 mm, green; d_0 = 0.70 mm, blue; d_0 = 0.90 mm, yellow).

7. Discussion

The derived formulas and the simulation example indicate the extent of vibration damping and natural frequency shift (de-tuning) of a realistic system. In contrary to idealistic simulations in previous first author's papers (Stein et al., 2011 and 2012) the presented paper consequently accounts for the coil electrical properties. This is a better approximation of the real situation; however, still some simplifications have been introduced in the course of analysis to make the problem tractable:

- Simplification of the magnetic force description by Eq. (9). Especially the material magnetic non-linearity, fringing effects and magnetic field non-uniformity may affect the system dynamic properties. This is seen in e.g. the discrepancy of the linear magnetic force air gap width relation of formula (35) and the real measured response, depicted in Fig. 3. More adequate description of this relation would call for more measurements and a better approximation of the measured data by a non-linear relation. This is especially true for small air gap width.
- The assumption that the beam transversal vibrations can be approximated by a SDOF oscillatory system, describing the beam mid-point oscillations at its first eigenfrequency may be too simple. Higher eigenfrequencies may be excited. Hence, a more complex model of the beam-actuator interaction has to be designed. Also the simplifications in the course of derivation of the Eq. (31) might have been to optimistic.

There are reports of using electromagnetic actuator as a device for de-tuning of *a cantilever beam* natural frequency, as described in Gospodarič et al. (2007); Brezina et al. (2011) and Belhaq et al. (2011). This is possible by changing the distance d_0 between the beam and the PM, as illustrated in Fig. 6 for *a clamped-clamped beam*, or more favourably, by replacing the PM by an electro-magnet energised by a controllable DC current, as proposed by the first author elsewhere. Variation in the magnetic stiffness k_M and corresponding decrease in the system first eigenfrequency from $\Omega = 1$ up to $\Omega = (1 - \kappa/2)^{1/2}$ is possible, as follows from Eq. (32). This effect is often regarded as the introduction of the 'negative stiffness' into the oscillatory system and used in vibration control.

8. Conclusion

Based on the developed theory and some preliminary measured data for the particular permanent magnet with coil and a realistic machine chassis, the advantage of use of a permanent magnet with a coil as a vibration controller is exploited. Using an external resistance R_S the original system natural frequency can be lowered to some extent, i.e. the oscillatory system natural frequency can be de-tuned, depending on the air gap width d_0.

Acknowledgement

This contribution is a result of the project No. 2/0083/13 of the Slovak VEGA Grant Agency.

References

Belhaq, M., Bichri, A., Der Hogapian, J. & Mahfoud J. (2011) Effect of electromagnetic actuations on the dynamics of a harmonically excited cantilever beam. *Intl. J. of Non-Linear Mechanics,* 46, 6, pp. 828-833.

Bishop, R.H., ed. (2002) *The Mechatronics Handbook.* CRC Press, Boca Raton.

Brezina, T., Vetiska, J., Hadas, Z. & Brezina, L. (2011) Simulation Modelling and Control of Mechatronic Systems with Flexible Parts, in: *Proc. 9th Int.Conf. Mechatronics 2011* (R. Jablonski & T.Brezina eds), Springer Verlag, Berlin, pp. 569-578.

Frank, L. et al. (1973) *Mathematics (In Czech).* SNTL, Prague.

Giurgiutiu, V. & Lyshewski, S.E. (2009) *Micromechatronics: Modeling, Analysis and Design*. 2nd ed., CRC Press, Boca Raton.

Gospodarič, B., Vončina, D. & Bučar, B. (2007) Active electromagnetic damping of laterally vibrating ferromagnetic cantilever beam. *Mechatronics,* 17, 6, pp. 291-298.

Harris, C. M. & Creede, E. C. (1961) *Shock and Vibration Handbook*. 3rd ed., McGraw-Hill, New York.

Cheng, T.-H. & Oh, I.-K. (2009) A current-flowing electromagnetic shunt damper for multi-mode vibration control of cantilever beams. *Smart Materials and Structures*, 18, 9, art. no. 095036 (10pp).

Mayer, D. & Ulrych, B. (2009) *Elektromagneticke aktuatory (in Czech).* BEN, Prague.

Niu, H. X., Xie, S. & Wang, P. (2009) A new electromagnetic shunt damping treatment and vibration control of beam structures. *Smart Materials and Structures*, 18, 4, art. no. 045009 (15pp).

Preumont, A. (2011) *Vibration Control of Active Structures.* 3rd ed., Springer, Berlin.

Stein, G. J., Darula, R. & Sorokin, S. (2011) Control of transversal vibrations of a clamped-clamped beam by a permanent magnet and a shunt circuit. in: *Proc. of the 8th intl. Conference on Structural Dynamics (EuroDyn 2011).* Katholieke Universiteit Leuven, Department of Civil Engineering, 2011, pp. 1735-1741.

Stein, G. J., Darula, R. & Sorokin, S. (2012) Control of forced vibrations of mechanical structures by an electromagnetic controller with a permanent magnet. in: *Proceedings International Conference on Noise and Vibration Engineering (ISMA 2012),* Katholieke Universiteit Leuven, Dept. Werktuigkunde, pp. 385-393.

Xu, X. & Zhu, S. (2010) A Magnetic Force Spring and its Application in Driver's Seat Suspension. in: *Intl. Conf. on Mechanic Automation and Control Engineering (MACE2010),* Wuhan, P.R. China, 26-28 June 2010. art. no. 5535656 (3 pp).